

Molecular Physics

An International Journal at the Interface Between Chemistry and Physics

ISSN: 0026-8976 (Print) 1362-3028 (Online) Journal homepage: <http://www.tandfonline.com/loi/tmph20>


Bonding in the metallic molecular solid α -Gallium

Richard C. Remsing, Jianwei Sun, Umesh V. Waghmare & Michael L. Klein


To cite this article: Richard C. Remsing, Jianwei Sun, Umesh V. Waghmare & Michael L. Klein (2018) Bonding in the metallic molecular solid α -Gallium, Molecular Physics, 116:21-22, 3372-3379, DOI: [10.1080/00268976.2018.1487598](https://doi.org/10.1080/00268976.2018.1487598)

To link to this article: <https://doi.org/10.1080/00268976.2018.1487598>

 View supplementary material 

 Published online: 22 Jun 2018.

 Submit your article to this journal 

 Article views: 28

 View Crossmark data 

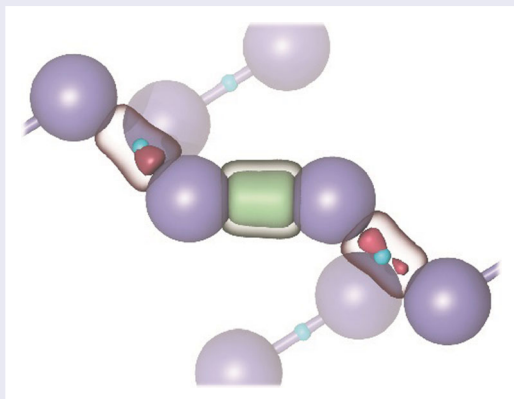
Bonding in the metallic molecular solid α -Gallium

Richard C. Remsing^a, Jianwei Sun^b, Umesh V. Waghmare^c and Michael L. Klein^a

^aInstitute for Computational Molecular Science and Department of Chemistry, Temple University, Philadelphia, PA, USA; ^bDepartment of Physics and Engineering Physics, Tulane University, New Orleans, LA, USA; ^cJawaharlal Nehru Center for Advanced Scientific Research, Bangalore, India

ABSTRACT

Solid, liquid and alloyed phases of gallium play a role in a variety of important technological applications. While many of the gallium phases involved in these applications are metallic, some have been proposed or are known to contain covalently bound Ga dimers. Thus, understanding the nature of bonding in Ga is crucial to the development of Ga-based materials. The solid phase of gallium at ambient conditions, α -Ga, is metallic and composed of molecular dimers, and can serve as a testing ground for studying gallium bonding with electronic structure calculations. We use density functional theory-based molecular dynamics simulations in conjunction with maximally localised Wannier functions to examine the nature of chemical bonding in α -Ga. We propose a geometric criterion for defining various bonding environments, which enables the quantification of covalent and weak bonds in solid gallium. We additionally connect the bonding structure of α -Ga to its phonon density of states and discuss similarities and differences with diatomic halogen crystals.



ARTICLE HISTORY

Received 5 March 2018
Accepted 31 May 2018

KEYWORDS

Ab initio molecular dynamics simulations; SCAN; density functional theory; maximally localised Wannier functions; chlorine


1. Introduction

Gallium is increasingly utilised in a wide range of applications. Heterogeneous nanostructures based on gallium nanoparticles show promise in many plasmonic technologies [1–3]. Gallium is also finding importance in the development of phase change memory materials [2,4,5]. Recently, a two-dimensional analog of α -Ga was synthesised, which has unique electronic structure and promises to serve as an important component of novel nanoscale devices [6]. When melted, liquid gallium has found use as a catalyst in a variety of applications, including nanotube fabrication [7], and has shown

promise as a liquid phase solvent for the synthesis of atomically thin materials [8].

In all of these applications, the unique structural properties of gallium are expected to play an important role. In particular, the metallic solid α -Ga phase is composed of layers of covalently bound Ga dimers [9–12] that adopt a unique orthorhombic structure, shared with the halogen crystals Cl₂, Br₂ and I₂ [9,13–17]. The other metallic phases of solid Ga are dominated by metallic bonds and do not consist of covalently bound molecular species. The Ga dimers have been postulated to persist into the liquid state [18], although this has been debated [12,19].

CONTACT Richard C. Remsing  rresing@temple.edu; Michael L. Klein  mike.klein@temple.edu  Institute for Computational Molecular Science and Department of Chemistry, Temple University, Philadelphia, PA 19122, USA

 Supplemental data for this article can be accessed here. <https://doi.org/10.1080/00268976.2018.1487598>

The ability of Ga to form molecular dimers that dissociate or weaken upon phase transformation may be critical to understanding the chemistry underlying many of the technological applications of Ga.

Mixed metallic-covalent systems, like α -Ga, can be expected to pose a challenge to methods for describing the electronic structure of the system, including density functional theory (DFT)-based approximations. In particular, the density functional approximation used to describe the system must be able to accurately describe highly localised electronic environments typical of covalent bonds while also yielding a good description of the diffuse electronic structures typical of metallic systems, in addition to any interplay between these two limits. Perhaps surprisingly, past work has shown that the simplest local density approximation (LDA) can provide a reasonable description of the molecular and electronic structure of α -Ga [9,11].

We revisit this problem by comparing the results of the LDA to the newly developed strongly constrained and appropriately normed (SCAN) meta-generalised gradient approximation (meta-GGA) [20,21], including a non-local van der Waals (vdW) correction (rVV10) [22]. The SCAN density functional has been shown to recognise and describe virtually all types of bonds with good accuracy, including covalent, metallic and even intermediate-range vdW bonds [21,23], all of which are expected to be significant in α -Ga. Thus, we expect the SCAN density functional to accurately capture the coexistence of covalent and metallic bonding in α -Ga. For large polarisable atoms like Ga, one might expect long-ranged vdW interactions to be significant near ambient conditions, and we also consider the influence of the rVV10 vdW correction on the structure of α -Ga. Despite these expectations, the SCAN-based results detailed herein indicate underperformance of this approach, which we attribute to deficiencies of the basis sets and pseudopotentials currently available, and not the SCAN density functional approximation itself, as discussed below and in the Supplemental Material.

In this work, we examine the nature of covalent bonding in α -Ga through the use of maximally localised Wannier functions (MLWFs) [24]. MLWFs are obtained from the periodic Bloch functions through a unitary transformation and serve as the solid-state equivalent of molecular orbitals [24]. Consequently, MLWFs have proved advantageous to quantify chemical bonding in periodic systems, including disordered liquids and crystalline and amorphous solids [24–30]. We examine the correlations between Ga atoms and MLWF centers, culminating in geometric criteria for defining specific classes of bonds in α -Ga, namely covalent, weak and non-bonded species. We use these bonding definitions to quantify the nature

of chemical bonding in α -Ga and use this knowledge to understand the dependence of the phonon density of states (DOS) on temperature and on the density functional used to describe the system, comparing the LDA and SCAN density functionals. We anticipate that our general approach can be readily extended to understand chemical transformations in other, more complex Ga-based systems.

2. Simulation details

All calculations employed the CP2K package, and energies and forces were evaluated using the QUICKSTEP module [31]. QUICKSTEP employs basis sets of Gaussian-type orbitals and plane waves for the electron density, leading to an efficient and accurate implementation of DFT [32]. We employ the shorter-range molecularly optimised (MOLOPT) Godecker–Teter–Hutter (GTH) double- ζ , single polarisation (DZVP-MOLOPT-SR-GTH) basis set [32] and the GTH-PADE (LDA-based) pseudopotential [33] to represent the core electrons of Ga. The $3d^{10}4s^24p^1$ electrons were treated explicitly, using the LDA as implemented in CP2K or the SCAN functional as implemented in LIBXC version 4.0.1 [34,35], with a plane wave cutoff of 750 Ry. The rVV10 vdW correction was employed as implemented in CP2K with the input parameters developed for use with SCAN [22]. A constant temperature of $T = 200$ K or $T = 300$ K was maintained using a Nosé-Hoover thermostat chain of length three [36,37] with an integration timestep of 1.0 fs. Systems were equilibrated for at least 4 ps before gathering statistics over at least 4 ps of production simulation time. MLWFs were obtained using CP2K, minimising the spreads of the MLWFs according to the formulation of [38].

We also performed density functional calculations for solid chlorine to compare the bonding structure to Ga. We treat the $3s^23p^7$ electrons explicitly. All other aspects of the calculations follow those given above for Ga, replacing the Ga pseudopotentials and basis sets with their analogs for chlorine.

3. Equation of state

We first examine the equation of state of α -Ga via static electronic structure calculations. Specifically, we compute the energy as a function of the system volume for a $3 \times 3 \times 2$ supercell consisting of 144 atoms. The geometry of the system is relaxed at each volume, while the cell vectors are held fixed. Moreover, we do not deform the individual lattice vectors independently. Instead, we fix the relative lattice vectors at the experimental values

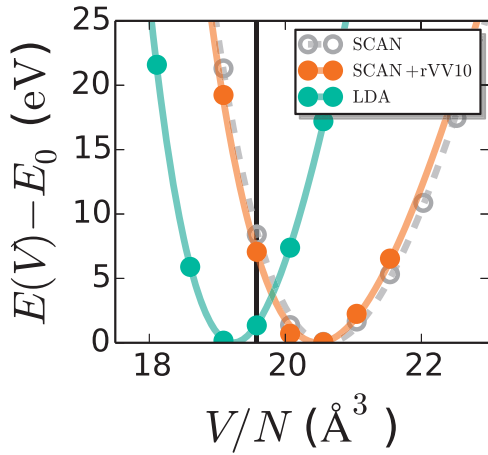


Figure 1. Equation of state, $E(V)$, of α -Gallium computed within the SCAN meta-GGA, the vdW-corrected SCAN+rVV10 meta-GGA, and the LDA, shown as data points. The vertical solid line corresponds to the experimental value of the specific volume. Lines indicate fits to the Murnaghan equation of state.

and simply scale all lattice vectors equally when changing the volume. The equation of state, $E(V)$, determined here with the LDA, SCAN and SCAN+rVV10 functionals, are fit well to the Murnaghan equation of state [39], as shown in Figure 1, enabling the determination of the specific volume of α -Ga in each system.

The SCAN functional overestimates the specific volume of α -Ga, with $V_{\text{SCAN}}/N \approx 20.60 \text{ \AA}^3$, compared to the experimental value $V_{\text{Exp.}}/N = 19.58 \text{ \AA}^3$. This estimate is improved through the inclusion of vdW interactions within the rVV10 scheme, leading to $V_{\text{SCAN+rVV10}}/N \approx 20.48 \text{ \AA}^3$. In contrast, LDA underestimates the specific volume, with $V_{\text{LDA}}/N \approx 19.23 \text{ \AA}^3$, indicating overbinding. These results were obtained by fixing the relative sizes of the lattice vectors equal to those determined experimentally. Distortion of the vectors and their relative orientation may lead to better agreement with the experimental volume, but only through a cancellation of errors in the various lattice vectors and their relative orientations. We also emphasise that the results in Figure 1 are obtained in a static system (0 K), and the inclusion of phonon modes will tend to increase the volume of the system.

4. Molecular structure of α -Ga

We simulate α -Ga at $T = 200 \text{ K}$ and $T = 300 \text{ K}$ with the latter being close to the experimental melting point of $T_m \approx 303 \text{ K}$. All simulations are performed at the minimum energy volume determined in Figure 1, unless otherwise noted, focusing on the LDA and SCAN+rVV10 systems. The different specific volumes predicted by LDA, SCAN and SCAN+rVV10 lead to appreciable

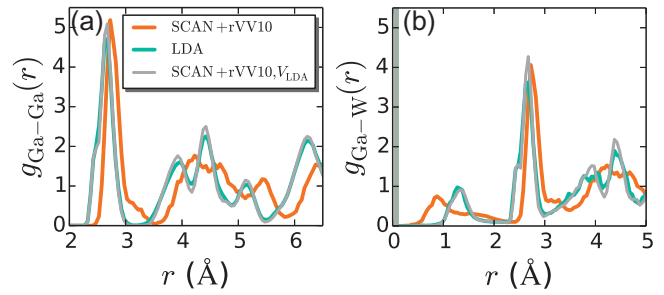


Figure 2. Radial distribution functions, $g(r)$, characterising (a) Ga-Ga and (b) Ga-W correlations, where W indicates the centre of a MLWF. Results are shown for SCAN+rVV10, LDA and SCAN+rVV10 at V_{LDA} at $T = 200 \text{ K}$.

changes in the structure of α -Ga, as illustrated by the radial distribution functions, $g(r)$, shown in Figure 2(a) for $T = 200 \text{ K}$. The lower specific volume of LDA leads to a first peak in the Ga-Ga $g(r)$ at smaller distances than that predicted by SCAN and SCAN+rVV10. Consequently, the subsequent peaks in $g(r)$ at larger distances are sharper and more well defined, indicating that the LDA system is slightly more ordered; note that all systems are still crystalline solids.

The Ga-W $g(r)$ is shown in Figure 2(b) for both the LDA and SCAN+rVV10 descriptions of the system, where W indicates the centre of a MLWF. Many of the MLWFs, associated with the d -orbitals, are highly localised close to the nuclei, giving rise to a large peak very close to the origin. This additionally leads to significant regions of $g_{\text{Ga-W}}(r)$ that closely track the correlations between nuclei captured by $g_{\text{Ga-Ga}}(r)$.

A peak is observed in $g_{\text{Ga-W}}(r)$ between 0.5 and 2 \AA , that may, at least in part, be ascribed to covalent bonding. For LDA, a well-defined peak is centred around 1.3 \AA , which is roughly half of the location of the first peak in $g_{\text{Ga-Ga}}(r)$, consistent with this peak arising from electrons involved in Ga-Ga bonds. The SCAN description of Ga-W correlations is more complex. The first peak in $g_{\text{Ga-W}}(r)$ is located near 0.88 \AA , and a broad shoulder spanning from this distance to more than 2 \AA is observed.

The asymmetry of the first peak in $g_{\text{Ga-W}}(r)$ predicted by SCAN+rVV10 is coupled to the expanded volume of the system, in comparison to the LDA case. Simulation of α -Ga with SCAN+rVV10 at V_{LDA} leads to a Ga-W correlation function, and Ga-Ga correlation function, that closely mimics that of the LDA system, as shown in Figure 2, although the first Ga-Ga peak in the SCAN+rVV10 system is slightly larger than that of LDA at the same volume. Thus, this complex electronic structure is closely coupled to the volume deformations of the system. Such asymmetric peaks can originate from a number of sources, including covalent bonds, polarised

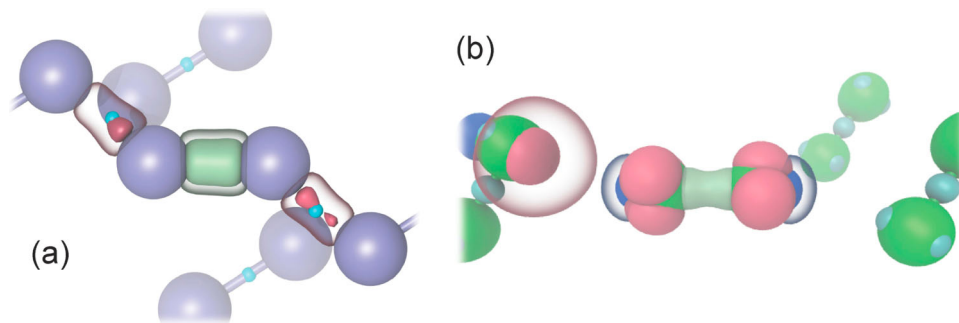


Figure 3. (a) MLWFs in α -Ga, focusing on a representative Ga₂ dimer (horizontal, centre) and its two nearest neighbour dimers (leftmost and rightmost Ga atoms); two other Ga₂ dimers and the MLWF centers of their covalent bond are shown in the background. The Ga-Ga dimer bond length is 2.447 Å. Gallium atoms are indicated by large spheres, which are connected by a cylinder to indicate Ga₂ dimers, and the centres of the MLWFs are drawn as small spheres. The MLWF of the covalent Ga₂ bond is shown in the centre of the figure, while those connecting dimers are to the left and right of the centre-most dimer. Two isosurfaces are shown for each MLWF: solid surfaces are drawn at 0.14 Bohr⁻³ and transparent surfaces are drawn at 0.12 Bohr⁻³. (b) MLWFs in solid Cl₂, focusing on a representative dimer (horizontal, centre) and its two nearest neighbour dimers; one Cl₂ dimer and its associated MLWF centers are shown in the background. The bond length of the Cl-Cl dimer is 2.017 Å. Cl atoms are shown as large spheres and MLWF centers as small spheres. The covalent bond MLWF is the isosurface at the centre of the figure and the three lone pair MLWFs are the spherical cap-like isosurfaces on each Cl atom; both are drawn at 0.22 Bohr⁻³. The remaining isosurfaces, along the bond axis and opposite the lone pair of the left-most dimer, indicate MLWFs that correspond to electron deficient regions, drawn at 0.08 Bohr⁻³. Transparent surfaces highlight MLWFs involved in an electrostatic, halogen bond, and are drawn at a lower isosurface density of 0.05 Bohr⁻³. The structure of Cl₂ is that determined experimentally [40]. Results are shown for LDA predictions; SCAN yields qualitatively similar results.

bonds and lone pairs. To understand the origins of the first peak in $g_{\text{Ga-W}}(r)$, we need to delve deeper into the electronic structure of α -Ga, particularly through examination of the MLWFs and higher order correlations involving the MLWF centers.

4.1. Wannier function-based bonding analysis

MLWFs (isosurfaces) and their centers (small spheres) surrounding a Ga₂ dimer are shown in Figure 3(a). We find that there are two major types of MLWF centers around a dimer. One MLWF centre appears on a line connecting the two Ga atoms involved in the dimer, as illustrated by the two dimers shown in the background of Figure 3(a). The corresponding MLWF indicates the formation of a covalently bonded Ga₂ dimer.

Each dimer also has two MLWF centers found between each of its Ga atoms and a Ga atom of a neighbouring dimer. Each of these MLWF centers is slightly off the line connecting the two Ga atoms, as shown on the left and right sides of Figure 3(a) and discussed in more detail below. The corresponding MLWF is drawn at two isosurfaces, one at high and low density, as is that corresponding to the covalent Ga₂ bond. At low isosurface density, the MLWF connects the two neighbouring Ga₂ dimers and suggests covalent bond formation. However, high isosurface density renderings of the MLWF suggests an electrostatic interaction typical of lone pairs; the MLWF does not span the region between the two Ga atoms and is instead localised near that of the central dimer. Note that the Ga₂ covalent bond MLWF does not qualitatively

change at these two isosurface levels. This analysis suggests that a weaker, directional interaction, with partial covalent or charge transfer character, may exist between Ga₂ dimers in α -Ga. These weaker interactions can also be observed through examination of the charge density of the system, as shown in previous work [9,18].

Analogous bonding arrangements are also observed in the solid phase of halogen molecules, such as Cl₂ and I₂, which share the same orthorhombic crystal structure as α -Ga [9,13–17]. For comparison, we examined the MLWFs for solid Cl₂, which are shown in Figure 3(b). Packing of the lone pairs of halogen dimers, which conceptually lead to an anisotropic shape to the halogen dimer, play an important role in determining this non-trivial crystal structure [13–16]. Analysis of the electronic structure of solid chlorine and iodine has demonstrated that electron density is depleted at the ends of the dimers along the bond axis, as well as between the lone pairs of the halogen atom, forming a σ -hole at each location [16,17]. The lone pair region on one end of a dimer then pairs with the σ -hole of its neighbour, in a Lewis-type interaction, forming a halogen bond between two dimers [17,41]. Importantly, this halogen bonding interaction is purely electrostatic in origin, and the MLWFs characterising the Cl₂ inter-dimer interactions show no evidence for covalency, highlighted by the transparent surfaces in Figure 3(b). This differs from α -Ga (Figure 3(a)), where the MLWFs suggest weakly or partially covalent interactions between dimers, ultimately originating from the unoccupied molecular orbitals of Ga₂.

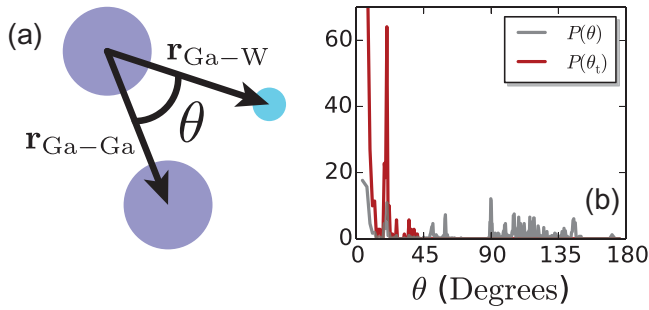


Figure 4. (a) Definition of the Ga-Ga-W angle, θ . Ga atoms and a MLWF centre are drawn as large and small circles, respectively. (b) Probability distributions of Ga-Ga-W angles in the α -Ga crystal obtained using distance constraints involving a single Ga atom, $P(\theta)$, or both Ga atoms in the triplet, $P(\theta_t)$. Both distributions are normalised to yield unity for an isotropic distribution. Results are for the energetic minimum as predicted by the LDA.

4.2. Wannier function-based bond definitions

To further understand the bonding structure captured by the radial distribution functions shown in Figure 2, we must quantify where each MLWF centre appears in $g_{\text{Ga-W}}(r)$. To accomplish this task, we examine three-body correlations between Ga atoms and MLWF centers, as captured by the probability distribution of the angle formed by each nearest neighbour Ga-Ga-W triplet, schematically illustrated in Figure 4(a). For a central Ga atom, a nearest neighbour Ga atom is defined as being a distance $r_{\text{Ga}} < 3 \text{ \AA}$ from the central Ga atom, and a nearest neighbour MLWF centre is within the range $0.15 \text{ \AA} < r_{\text{W}} < 1.75 \text{ \AA}$ from the central atom. A lower bound on the Ga-W distance is set to avoid counting those centers that are highly localised on the Ga atoms. The Ga-Ga-W angle computed in this manner is referred to as θ . We also examine a more tightly defined definition of this angle, θ_t , which requires that the MLWF centre is within the range $0.15 \text{ \AA} < r_{\text{W}} < 1.75 \text{ \AA}$ from both Ga atoms involved in the Ga-Ga-W triplet.

The angular distributions in the energy minimised LDA structure are shown in Figure 4(b). Using the single Ga atom distance criteria, $P(\theta)$ has many peaks spanning nearly the entire range of θ , with small regions of negligible probability, like that between roughly 65° and 90° . Triplets forming large Ga-Ga-W angles are not involved in bond formation, as the MLWF centers are not located between the two Ga atoms of interest.

Including the additional distance constraints involving the second Ga atom results in $P(\theta_t)$ being non-zero for $\theta_t < 45^\circ$. This distribution features two major peaks, one near $\theta_t = 0^\circ$ and one near $\theta_t = 20^\circ$. The peak at $\theta_t = 0^\circ$ corresponds to the linear, covalent bonds of the Ga_2 dimers. As discussed above, the MLWF centers located between two pairs of dimers are not on the line

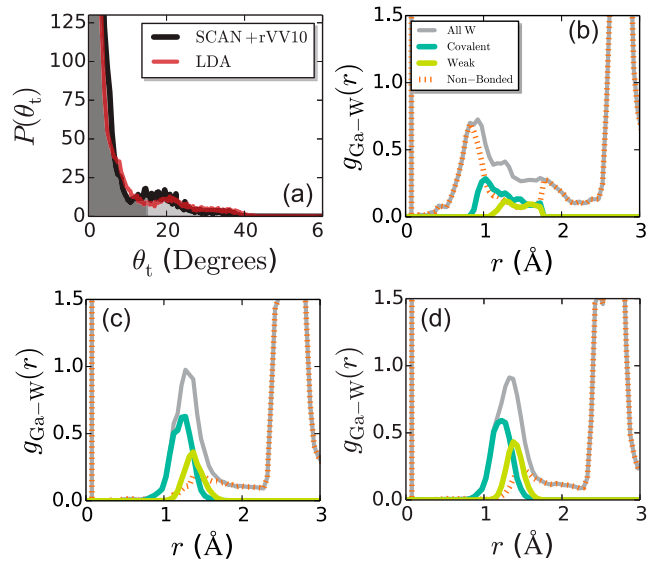


Figure 5. (a) Probability distributions of Ga-Ga-W angles in the α -Ga crystal obtained using distance constraints involving both Ga atoms in the triplet, $P(\theta_t)$, for the LDA and SCAN+rVV10 systems. Both distributions are normalised to yield unity for an isotropic distribution. Dark and light shaded region indicates covalent bond and weak bond angles. (b,c,d) Radial distribution functions for Ga-W correlations decomposed according to whether the MLWF centre is involved in a covalent bond, a weak bond, or neither (non-bonded), shown for (b) SCAN+rVV10, (c) LDA and (d) SCAN+rVV10 at V_{LDA} .

connecting two Ga atoms, Figure 3(a). These MLWF centers lead to the appearance of the peak at $\theta_t = 20^\circ$ in $P(\theta_t)$, and correspond to the relatively weaker interactions between neighbouring Ga_2 dimers.

The above analysis enables us to propose a criterion for defining various bonds in α -Ga. If two Ga atoms are separated by a distance less than 3 \AA (the first minimum in $g_{\text{Ga-Ga}}(r)$), and the Ga-Ga-W angle involving these atoms is $\theta_t < 15^\circ$ (the first minimum in $P(\theta_t)$), these two Ga atoms are covalently bonded to form a Ga_2 dimer. If two Ga atoms are separated by a distance less than 3 \AA , and the corresponding Ga-Ga-W angle is $15^\circ \leq \theta_t < 30^\circ$, these two Ga atoms are involved in a weaker, partially covalent interaction typical of those between dimers, as shown on the left and right of Figure 3(a). Otherwise, the two Ga atoms are not bonded.

4.3. Bonded and non-bonded correlations

Using the above definition of bond types, we can quantify where the MLWF centers of each bonding environment contribute to $g_{\text{Ga-W}}(r)$. First, we note that the probability distribution $P(\theta_t)$ for both LDA and SCAN+rVV10 at finite T are similar to that in the $T=0 \text{ K}$ lattice, Figure 5(a). Both distributions have a large peak

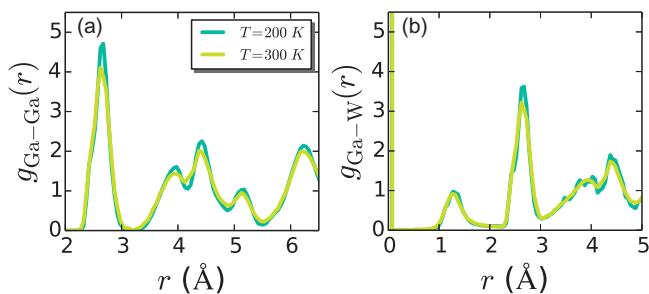


Figure 6. Radial distribution functions, $g(r)$, characterising (a) Ga-Ga and (b) Ga-W correlations, where W indicates the centre of a MLWF, at $T = 200$ K and $T = 300$ K for LDA at fixed volume.

near $\theta_t = 0^\circ$, corresponding to covalent bonds, and a secondary peak near $\theta_t = 20^\circ$, indicative of weak bonding between Ga_2 dimers. Therefore, the above-defined bonding criterion should be sufficiently general to quantify bonding at finite T , and the regions of θ_t consistent with covalent and weak bonds are highlighted by the dark and light shaded regions of Figure 5(a), respectively.

Using these bonding definitions, we split Ga-W pair distribution functions into contributions from MLWF centers that correspond to Ga_2 dimer covalent bonds, weak bonds between Ga atoms, and non-bonded interactions between Ga atoms,

$$g_{\text{Ga-W}}(r) = g_{\text{Ga-W}}^{\text{Covalent}}(r) + g_{\text{Ga-W}}^{\text{Weak}}(r) + g_{\text{Ga-W}}^{\text{Non-Bonded}}(r). \quad (1)$$

The components of $g_{\text{Ga-W}}(r)$ obtained in this way are shown in Figure 5(b,c) for the SCAN+rVV10 and LDA systems, respectively. In both cases, the peak between 0.5 and 2 Å is composed of MLWF centers involved in all types of bonding environments, not just covalent bonds. This highlights the importance of considering higher order correlations when using MLWF centers to quantify molecular bonding; here we use triplet correlations in addition to pair correlations involving two Ga atoms and a MLWF centre. Moreover, we find that bonding is less prevalent in the expanded α -Ga system produced by SCAN and SCAN+rVV10. As discussed above, this is mainly an effect of the increased volume, not functional. At the same volume, LDA and SCAN+rVV10 yield similar descriptions of the molecular structure of α -Ga, Figure 5(d).

We conclude our structural analysis with a discussion of the temperature dependence of the Ga-Ga and Ga-W correlations at constant volume. The radial distribution functions obtained via LDA at $T = 200$ K and $T = 300$ K are shown in Figure 6 and indicate that the structure of α -Ga changes very little over this temperature range when the volume is held fixed. The first peak in $g_{\text{Ga-Ga}}(r)$

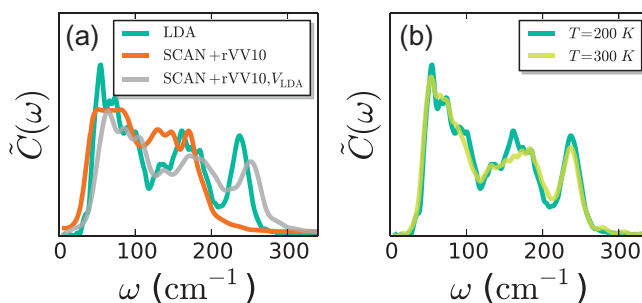


Figure 7. (a) Phonon DOS, $\tilde{C}(\omega)$, of α -Ga as predicted by LDA, SCAN+rVV10 and SCAN+rVV10 at V_{LDA} . (b) Temperature dependence of $\tilde{C}(\omega)$ for the LDA system at fixed volume.

decreases slightly, and the remaining peaks are broadened slightly by the enhanced thermal motion at high T . Similar broadening is observed for the peaks in $g_{\text{Ga-W}}(r)$ that mimic the Ga-Ga correlations. Importantly, the peak in $g_{\text{Ga-W}}(r)$ between 0.5 and 2 Å that contains the covalent bonding MLWF centre correlations is unchanged as the system is heated along an isochore, suggesting that the covalent Ga_2 dimers remain intact even at temperatures close to the melting point.

5. Molecular dynamics of α -Ga

The differences in covalent bonding produced by the various treatments of α -Ga discussed above manifest in the dynamic properties of the solid. Here, we focus on the phonon DOS, $\tilde{C}(\omega)$, as obtained from the Fourier transform of the velocity autocorrelation function [42]

$$C(t) = \langle \mathbf{v}(t) \cdot \mathbf{v}(0) \rangle, \quad (2)$$

where $\mathbf{v}(t)$ indicates the velocity vector of an atom at time t and implicit in the notation is an average over all atoms in the solid. The phonon DOS obtained for LDA, SCAN+rVV10 and SCAN+rVV10 at V_{LDA} are shown in Figure 7(a).

The phonon DOS for the LDA system displays three major features: a peak near 60 cm^{-1} , a broad peak near 160 cm^{-1} and a high frequency peak at 237 cm^{-1} . We attribute the latter, high frequency peak to the stretching mode of Ga_2 , and the frequency of this peak is in good agreement with that observed experimentally [12], 246 cm^{-1} . In the SCAN+rVV10 system, this peak shifts to a frequency of approximately 170 cm^{-1} , close to that determined experimentally for isolated Ga_2 dimers in an argon matrix [43], 177.4 cm^{-1} . This is consistent with the Ga-Ga bond length increasing from 2.447 Å in the LDA description of α -Ga, in good agreement with previous estimates for the solid phase [44,45], to 2.608 Å with SCAN+rVV10, which is closer to the isolated Ga_2 dimer bond distance of 2.75 Å [46,47]. Moreover, these results

are also consistent with the MLWF-based picture of a lower prevalence of strong covalent Ga₂ bonds and weakening of secondary (weak) inter-dimer interactions in the expanded volume SCAN+rVV10 system, discussed above (Figure 5).

The high frequency peak is recovered when simulating the system at V_{LDA} with SCAN+rVV10, indicating that this peak shift is primarily a volumetric effect. The phonon DOS for SCAN+rVV10 and LDA, both at V_{LDA} , are qualitatively very similar, as might be expected by comparing the structure in the two systems. In fact, the slight increase in bonding character of SCAN+rVV10, in comparison to LDA at the same volume, leads to a concomitant increase in frequency of the Ga₂ stretching mode to approximately 251 cm⁻¹, as evidenced by the phonon DOS in Figure 7(a).

Finally, we examine the temperature dependence of the phonon DOS at fixed volume. Under these conditions, changes in $\tilde{C}(\omega)$ are indicative of anharmonic effects. The computed $\tilde{C}(\omega)$ are essentially independent of temperature between $T=200$ K and $T=300$ K, as shown in Figure 7(b), which may be expected from the insensitivity of the bonding structure of α -Ga to changes in temperature at fixed volume. This also suggests that α -Ga behaves as a harmonic crystal. We additionally note that the dominant effect of temperature on $\tilde{C}(\omega)$ is usually through thermal expansion. While we do not examine this explicitly by allowing the volume to change with temperature, our results for SCAN+rVV10 at two volumes suggests that the Ga-Ga stretching mode is sensitive to volumetric changes and shifts to lower frequencies as the volume is increased. Additionally, the computed $\tilde{C}(\omega)$ for the SCAN functional without the rVV10 correction (not shown), which has the largest volume of the studied systems, displays a Ga-Ga stretching peak near 133 cm⁻¹, consistent with this observation. Therefore, our results suggest that the Ga-Ga stretching mode will shift to lower frequencies upon thermal expansion.

6. Conclusions

We have carried out a MLWF-based analysis of bonding in the molecular, metallic solid α -Ga, suggesting a bonding structure analogous to that in molecular halogen crystals [14,16,17], with electrostatic halogen bonding between neighbouring dimers replaced by weakly covalent interactions between Ga₂ dimers. By analysing the distances and angles between Ga atoms and MLWF centers, we developed a simple geometric criterion to distinguish among covalent bonds indicative of Ga₂ dimers, weak bonds between dimers and non-bonded contacts. This criterion enables us to decompose the pair correlation function between Ga atoms and MLWF centers

according to bonding environment, highlighting that correlations which may naively be ascribed solely to bonds are actually due to a sum of all bonding types. The accuracy of this decomposition is supported by the computed phonon densities of states of each system. The phonon DOS display a pronounced peak for Ga-Ga stretching vibrational modes in systems with strong covalent bonds, and this peak shifts to lower frequencies at larger volumes, when bonding is less prevalent. We expect that the bonding analysis developed here will prove useful to quantify dimerisation in the liquid state and other disordered Ga environments, for example, to monitor chemical transformations during nonequilibrium transitions in cycling of phase change memory materials [2,4,5,30,48,49]. Moreover, the MLWF-based perspective on bonding used here can complement previous approaches to revisit questions regarding bonding in molecular halogen crystals [16,17].

We conclude with a discussion of the limitations of our approach. In particular, we have found that the SCAN and SCAN+rVV10 density functional approximations provide a less accurate treatment of α -Ga than the simple LDA, largely due to inaccurate predictions of the density of the solid phase. Preliminary results indicate that the accuracy of such predictions is sensitive to the specific basis set and pseudopotential used to treat the electron density. Relatively few basis sets are available for Ga, and purely plane wave treatments yield very good estimates for the structure of α -Ga with SCAN, suggesting that the deficiencies found here arise from the basis set and not an inherent issue with the SCAN functional; see the Supplemental Material for more details. This suggests a need for SCAN-specific basis sets and pseudopotentials to accurately treat systems with complex electronic structure.

Acknowledgement

RCR thanks Chris Mundy (PNNL) for helpful discussions regarding CP2K. This article is dedicated to Daan Frenkel on the occasion of his 70th birthday.

Disclosure statement

No potential conflict of interest was reported by the authors.

Funding

This work was supported as part of the Center for the Computational Design of Functional Layered Materials, an Energy Frontier Research Center funded by the U.S. Department of Energy, Office of Science, Basic Energy Sciences under [Award #DE-SC0012575]. This research was supported in part by the National Science Foundation through major research instrumentation [grant number 1625061] and by the US Army Research Laboratory under [contract number W911NF-16-2-0189].

References

- [1] C. Yi, T.-H. Kim, W. Jiao, Y. Yang, A. Lazarides, K. Hingerl, G. Bruno, A. Brown, and M. Losurdo, *Small* **8**, 2721 (2012).
- [2] M.W. Knight, T. Coenen, Y. Yang, B.J.M. Brenny, M. Losurdo, A.S. Brown, H.O. Everitt, and A. Polman, *ACS Nano* **9** (2), 2049 (2015).
- [3] P.C. Wu, M. Losurdo, T.-H. Kim, M. Giangregorio, G. Bruno, H.O. Everitt, and A.S. Brown, *Langmuir* **25** (2), 924 (2009).
- [4] B.F. Soares, F. Jonsson, and N.I. Zheludev, *Phys. Rev. Lett.* **98**, (2007).
- [5] N.I. Zheludev, *J. Opt. A: Pure Appl. Opt.* **8** (4), S1 (2006).
- [6] V. Kochat, A. Samanta, Y. Zhang, S. Bhowmick, P. Manimunda, S.A.S. Asif, A. Stender, R. Vajtai, A.K. Singh, C.S. Tiwary, and P.M. Ajayan, *Sci. Adv.* **4**, e1701373 (2018).
- [7] J. Bae, J.B. Han, X.-M. Zhang, M. Wei, X. Duan, Y. Zhang, and Z.L. Wang, *J. Phys. Chem. C* **113** (24), 10379 (2009).
- [8] A. Zavabeti, J.Z. Ou, B.J. Carey, N. Syed, R. Orrell-Trigg, E.L.H. Mayes, C. Xu, O. Kavehei, A.P. O'Mullane, R.B. Kaner, K. Kalantar-zadeh, and T. Daeneke, *Science* **358** (6361), 332 (2017).
- [9] X.G. Gong, G.L. Chiarotti, M. Parrinello, and E. Tosatti, *Phys. Rev. B* **43**, 14277 (1991).
- [10] O. Züger and U. Dürig, *Phys. Rev. B* **46**, 7319 (1992).
- [11] M. Bernasconi, G.L. Chiarotti, and E. Tosatti, *Phys. Rev. B* **52**, 9988 (1995).
- [12] J.A. Creighton and R. Withnall, *Chem. Phys. Lett.* **326**, 311 (2000).
- [13] S.C. Nyburg and W. Wong-Ng, *Proc. R. Soc. Lond. A* **367**, 29 (1979).
- [14] E.D. Stevens, *Mol. Phys.* **37**, 27 (1979).
- [15] S.L. Price and A.J. Stone, *Mol. Phys.* **47**, 1457 (1982).
- [16] V.G. Tsirelson, P.F. Zhou, T.-H. Tang, and R.F.W. Bader, *Acta Cryst.* **51**, 143 (1995).
- [17] F. Bertolotti, A.V. Shishkina, A. Forni, G. Gervasio, A.I. Stash, and V.G. Tsirelson, *Cryst. Growth. Des.* **14** (7), 3587 (2014).
- [18] X.G. Gong, G.L. Chiarotti, M. Parrinello, and E. Tosatti, *Europhys. Lett.* **21**, 469 (1993).
- [19] J. Yang, J.S. Tse, and T. Iitaka, *J. Chem. Phys.* **135**, 044507 (2011).
- [20] J. Sun, A. Ruzsinszky, and J.P. Perdew, *Phys. Rev. Lett.* **115**, 036402 (2015).
- [21] J. Sun, R.C. Remsing, Y. Zhang, Z. Sun, A. Ruzsinszky, H. Peng, Z. Yang, A. Paul, U. Waghmare, X. Wu, M.L. Klein, and J.P. Perdew, *Nat Chem* **8**, 831 (2016).
- [22] H. Peng, Z.-H. Yang, J.P. Perdew, and J. Sun, *Phys. Rev. X* **6**, 041005 (2016).
- [23] R.C. Remsing, M.L. Klein, and J. Sun, *Phys. Rev. B* **96**, 024203 (2017).
- [24] N. Marzari, A.A. Mostofi, J.R. Yates, I. Souza, and D. Vanderbilt, *Rev. Mod. Phys.* **84**, 1419 (2012).
- [25] P.L. Silvestrelli, N. Marzari, D. Vanderbilt, and M. Parrinello, *Solid State Commun.* **107**, 7 (1998).
- [26] P.L. Silvestrelli and M. Parrinello, *Phys. Rev. Lett.* **82**, 3308 (1999).
- [27] T. Ogitsu, E. Schwegler, and G. Galli, *Chem. Rev.* **113** (5), 3425 (2013).
- [28] M. Sharma, Y. Wu, and R. Car, *Int. J. Quantum Chem.* **95** (6), 821 (2003).
- [29] A.R. Merchant, D.R. McKenzie, and D.G. McCulloch, *Phys. Rev. B* **65**, 024208 (2001).
- [30] T.H. Lee and S.R. Elliott, *Adv. Mater.* **29**, 4 (2017).
- [31] J. VandeVondele, M. Krack, F. Mohamed, M. Parrinello, T. Chassaing, and J. Hutter, *Comput. Phys. Commun.* **167**, 103 (2005).
- [32] J. VandeVondele and J. Hutter, *J. Chem. Phys.* **127**, 114105 (2007).
- [33] S. Goedecker, M. Teter, and J. Hutter, *Phys. Rev. B* **54**, 1703 (1996).
- [34] S. Lehtola, C. Steigemann, M.J. Oliveira, and M.A. Marques, *SoftwareX* **7**, 1 (2018).
- [35] M.A. Marques, M.J. Oliveira, and T. Burnus, *Comput. Phys. Commun.* **183** (10), 2272 (2012).
- [36] S. Nosé, *J. Chem. Phys.* **81**, 511 (1984).
- [37] S. Nosé, *Mol. Phys.* **52** (2), 255 (1984).
- [38] G. Berghold, C.J. Mundy, A.H. Romero, J. Hutter, and M. Parrinello, *Phys. Rev. B* **61**, 10040 (2000).
- [39] F.D. Murnaghan, *Proc. Natl. Acad. Sci. USA* **30** (9), 244 (1944).
- [40] S.C. Nyburg, *J. Chem. Phys.* **48**, 4890 (1968).
- [41] G. Cavallo, P. Metrangolo, R. Milani, T. Pilati, A. Priimagi, G. Resnati, and G. Terraneo, *Chem. Rev.* **116**, 2478 (2016).
- [42] M.L. Klein and L.J. Lewis, *Chem. Rev.* **90**, 459 (1990).
- [43] H.-J. Himmel and B. Gaertner, *Chem. Eur. J.* **10**, 5936 (2004).
- [44] N. Drebov, F. Weigend, and R. Ahlrichs, *J. Chem. Phys.* **135**, 044314 (2011).
- [45] N. Gaston and A. Parker, *Chem. Phys. Lett.* **501**, 375 (2011).
- [46] X. Tan and P.J. Dagdigian, *J. Phys. Chem. A* **15**, 2642 (2003).
- [47] R. Tonner and N. Gaston, *Phys. Chem. Chem. Phys.* **16** (44), 24244 (2014).
- [48] D. Loke, T.H. Lee, W.J. Wang, L.P. Shi, R. Zhao, Y.C. Yeo, T.C. Chong, and S.R. Elliott, *Science* **336** (6088), 1566 (2012).
- [49] J.M. Skelton, D. Loke, T. Lee, and S.R. Elliott, *ACS Appl. Mater. Interfaces* **7** (26), 14223 (2015).